ELSEVIER

Journal of Process Control 12 (2002) 131–141

JOURNAL OF PROCESS CONTROL

www.elsevier.com/locate/jprocont

Reduced complexity adaptive nonlinear control of a distributed collector solar field

M. Barão [a], J.M. Lemos [a,*], R.N. Silva [b]

[a] *INESC-ID/IST, Rua Alves Redol 9, 1000-029 Lisboa, Portugal*
[b] *FCT-UNL, Portugal*

Received 31 July 2000; received in revised form 18 December 2000; accepted 20 December 2000

Abstract

An approach to the control of a distributed collector solar field relying on feedback linearization, Lyapunov based adaptation and a simplified plant model is presented. The control objective consists of manipulating the oil flow so that the outlet oil temperature is regulated around a given setpoint. For dealing with plant nonlinearities and external disturbances, a nonlinear transformation is performed on the accessible variables such that the transformed system behaves as an integrator, to which linear control techniques are then applied. Since the transformation depends on an unknown parameter, an adaptation law is designed so as to minimize a Lyapunov function for the whole system's state. For the sake of control synthesis a simplified plant model which retains the bilinear nonlinearity is employed. The resulting control law has the same control structure of the one yielding exact input-output linearization but assumes a different placement of a temperature sensor. In order to justify this procedure, plant internal dynamics is studied. Experimental results obtained in the actual field are presented.

Keywords: Nonlinear control; Adaptive control; Solar energy; Distributed parameter

1. Introduction

This paper is mainly concerned with an experimental case study on adaptive nonlinear temperature control in a distributed collector solar field.

The field considered yields a power of 0.5 MW. It consists (Figs. 1 and 2) of a series of parabolic mirrors which concentrate solar radiation on a pipe, located along its focus, where oil gets heated while circulating. Fig. 3 (left) shows the detail of the solar collectors, where the pipe is seen as a white rod. In between every two collectors, the picture also shows the sensor of the automatic sun tracking system installed on the field. Fig. 3 (right) shows the deposit from which the oil to be heated is pumped from the bottom, through the field, and back to the top of the deposit. The thermal energy of the oil is extracted in another circuit and may be used either for water desalination or in a small thermoelectric unit. The objective of the control system is to maintain the outlet oil temperature at a desired level in spite of disturbances, such as changes in the solar radiation level, inlet oil temperature or optical efficiency of the mirrors caused e.g. by dust deposition. The manipulated variable is the oil flow (or, equivalently, oil velocity). More details can be found in Refs. [5–8].

Due to the degree of nonlinearities present, linear methods cannot perform well in this plant under all operating conditions. Fig. 4 shows the simulation of the response of the outlet oil temperature to a sequence of 20°C steps in the reference. These results were obtained by simulation on a distributed parameter model of the field. The controller used in this example is a constant gain PID with the gains selected according to the Takahashi rule [22], being optimized for $u = 4.5$, l/s. The proportional, integral and derivative gains are, respectively, $k_p = 0.053$, $k_I = 0.066$ and $k_D = 0.11$. As seen on Fig. 4, when the operating temperature increases, the response degrades and a steady oscillation appears.

Furthermore, plant parameters and in particular mirror optical efficiency may change unpredictably in time. Fig. 5 shows the daily evolution of the temperature at

* Corresponding author. Tel.: +351-21-310-0259; fax: +351-21-314-5843.

E-mail addresses: jlml@inesc.pt (J.M. Lemos), rns@mail.fct.unl.pt (R.N. Silva), mjsb@ramses.inesc.pt (M. Barão).

0959-1524/02/$ - see front matter
PII: S0959-1524(01)00003-8

the outlet of two different collector rows. While the oil flow and solar radiation are approximately the same for both rows, the time instant for which their temperature reaches the highest value differ noticeably. This is due to the fact that the shape of the collectors composing them is not exactly the same, thereby affecting the optical focus. It may even change unpredictably in time, due to wind or thermal mechanical stress. Dust deposition also affects optical efficiency. Although the nonlinearities could be compensated by using multiple linear controllers and gain-scheduling [11], the presence of uncertainty means that there is room for improvement with adaptive methods.

Fig. 1. A global view of the ACUREX solar collector field.

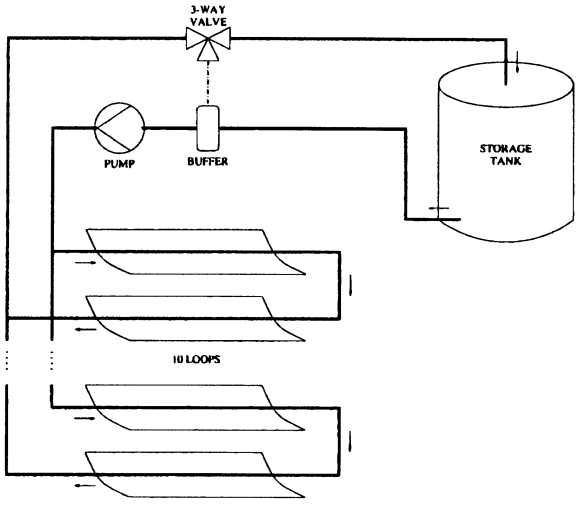

Fig. 2. Simplified diagram of the ACUREX field.

For tackling the above uncertainty effects, this paper resorts to an adaptive nonlinear controller based on feedback linearization [9,21], combined with Lyapunov based adaptation [8,10]. The basic idea consists in using the accessible variables from the plant to perform a transformation such that the new obtained system behaves approximately as a linear one. This transformation is derived from a simplified lumped parameter bilinear model which approximates a plant's distributed parameter model. The resulting equivalent linear system is then controlled by linear methods. The linear controller computes a new signal (called hereafter virtual control) which is transformed back and applied to the real plant. Since the transformation depends on an unknown parameter (optical efficiency), this is estimated on-line. For that sake, an adaptation law is designed for ensuring the semidefinite character of the time derivative of a candidate Lyapunov function.

By using a reduced complexity model, the step of feedback linearization becomes very simple. It remains to justify whether the approximations performed are valid. For that sake, it is shown that the resulting control law has the same structure of the one yielding exact input-output linearization but assumes a different placement of one of the temperature sensors. Also, a study of plant internal dynamics is made. Furthermore, experimental results obtained in the actual plant are presented in order to show that the transformed plant is actually close to an integrator.

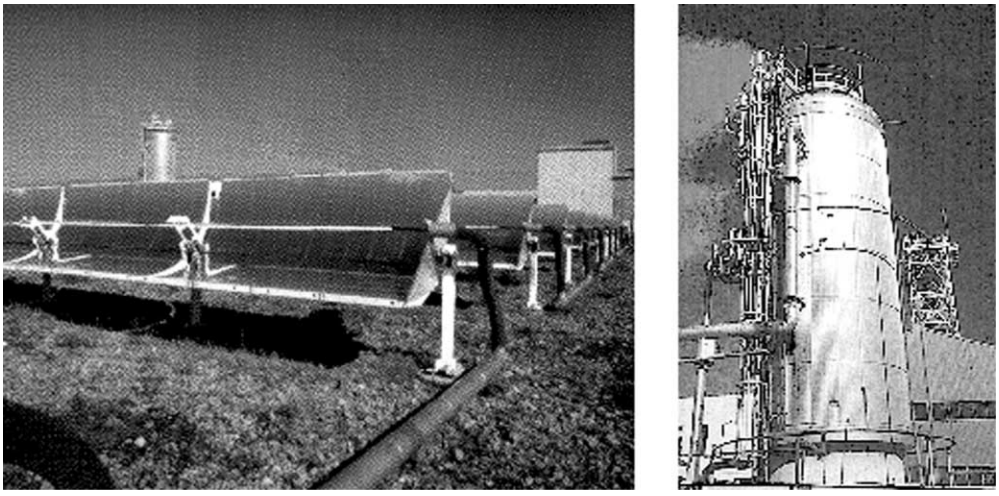

Fig. 3. Detail of the solar collectors (left) and the oil deposit.

The control of the plant considered has been the subject of several studies [3–8,12,17,18,20]. These include different types of adaptive predictive control strategies such as GPC [6], adaptive cascade control [20], fuzzy control [17], switching control [15] and other methods. The generality of the above works rely however on concentrated parameter models defined a priori and do not exploit the structure of the partial differential equation. In [7,12] a simplified analysis assuming the internal dynamics to be decomposable as a sum of sinusoids concludes that the plant presents anti-resonance characteristics and advantage is taken of this fact for control design.

The control of solar collector plants other than the one considered here but with a similar structure has been studied in [14,16] where an optimal control approach was followed. The problem is formulated in terms of a distributed parameter model, similar to the one considered in this paper. The solution relies on a maximum principle,

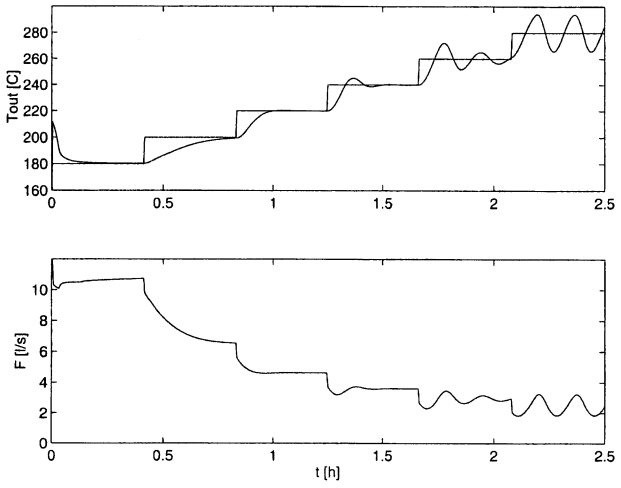

Fig. 4. Output temperature and reference (above) and manipulated variable (below) with a constant gain PID controller (simulation).

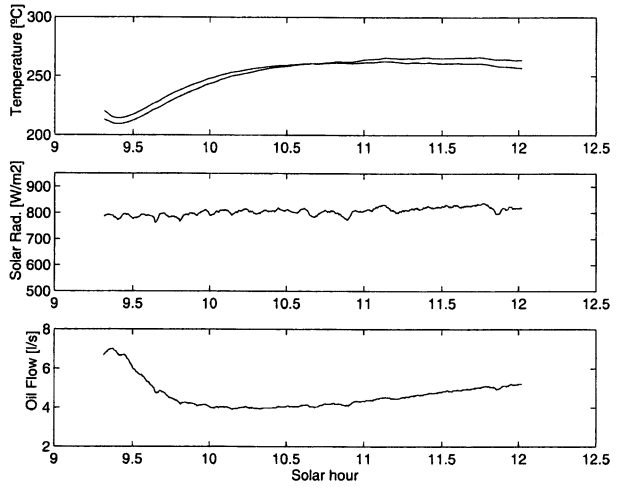

Fig. 5. Daily evolution of the temperature at the outlet of two collector rows.

together with the method of characteristics for partial differential equations. Both optimal and suboptimal bang-bang control strategies result. The control objectives in [14,16] are however substantially different from the ones considered in this paper and the other mentioned references. Opposite to [14,16], where a fixed optimisation horizon is sought, most of the work referred concerns the steady-state optimisation of a quadratic cost. Here, in particular, the control synthesis does not rely on the optimisation of a functional.

The approach followed in this paper is new with respect to the ones described above. Indeed, explicit use is made of the plant distributed parameter model, an approximation being made that simplifies control design while retaining the key aspects of plant nonlinear character. Furthermore, a detailed study is made of plant internal dynamics when the outlet oil temperature is constant. In this respect, it should be mentioned that [7,12] have obtained related (but not equal) results, using different methods and in a much different context. Although [16,14] derive their control law from the partial differential equation model, their formulation of the control problem is much different from the one considered here. The emphasis of this paper is to tackle plant uncertainty and parameter variations by the use of adaptive nonlinear methods together with simplified models.

Although solar energy is by itself an important issue, it is remarked that the approach followed here may in its generality be applied to other types of plants with a similar structure. Large heat exchangers and plug-flow tubular reactors controlled by variation of flow rate [19] provide examples.

The paper is organized as follows. Section 1 (this section) formulates and motivates the problem as well as its solution. The plant is shown not to be adequately controllable over a wide range of operating conditions by a constant gain PID. The control approach followed in this paper is explained, together with its novelty with respect to other previous works described in the literature. Section 2 concerns plant dynamics. A model for a single loop of the solar collector field is written in the form of a partial differential equation. By means of a space discretization, this is approximated by a lumped parameter bilinear model. Plant dynamics including plant equilibria and reachable states are discussed. In Section 3, input–output exact feedback linearization is obtained. Corresponding plant internal dynamics are discussed and compared with a modified control law to be used due to practical constraints. Section 4 addresses the problem of nonlinear adaptive control design. Motivated by the results in the previous section, a simplified model which corresponds to an approximation of the temperature space derivative is used as a basis for nonlinear adaptive control design. Section 5 presents experimental results obtained in the actual ACUREX field. In the first experiment, the linearization procedure

based on the simplified model is shown to be a reasonable approximation. In the second experiment the overall nonlinear adaptive control system is demonstrated. Finally, Section 6 draws conclusions.

2. Plant dynamics

Consider a single loop of the solar collector field. Given the small diameter of the pipe when compared to its length, and assuming incompressibility of the fluid and no diffusion, it is possible to model the temperature distribution along the pipe by a partial differential equation (PDE) of the form [5]:

$$\frac{\partial T(z,t)}{\partial t} + u(t)\frac{\partial T(z,t)}{\partial z} = \alpha R \tag{1}$$

where the following notation is used: $T(z,t)$ is the difference of oil temperature with respect to the inlet oil temperature (assumed constant), at each position z of the pipe and at time t, u is the manipulated variable oil speed (proportional to oil-flow), R is the corrected solar radiation and α is a parameter depending mainly on the optical efficiency of the mirrors. In the above model heat losses to the environment are not considered.

Assuming a smooth variation of oil temperature along the pipe, it is possible to approximate the temperature distribution by a piecewise linear curve, so that the following finite difference approximation holds:

$$\frac{\partial T}{\partial z}|_{z\in(z_{i-1},z_i]} \cong \frac{T_i - T_{i-1}}{h}, \quad i = 1, ..., n \tag{2}$$

where h is the length of each segment, n is the number of segments, $z_i = ih$, $L = nh$ is the pipe length and $T_i = T(ih,t)$.

Defining the state variables

$$x_i(t) = T(ih, t) \quad i = 1, ..., n \tag{3}$$

process dynamics is thus approximately described by the system of nonlinear ordinary differential equations:

$$\dot{x}_i = -u\frac{1}{h}(x_i - x_{i-1}) + \alpha R, \quad i = 1, ..., n \tag{4}$$

where the dot denotes derivative with respect to time t and $x_0 = 0$.

Defining the state $x = [x_1 ... x_n]^T$ and the vector fields

$$f(x) = \alpha R\begin{bmatrix}1\\1\\\vdots\\1\end{bmatrix} \qquad g(x) = -\frac{1}{h}\begin{bmatrix}x_1\\x_2 - x_1\\\vdots\\x_n - x_{n-1}\end{bmatrix}$$

system (4) is written in the form

$$\dot{x} = f(x) + g(x)u \tag{5}$$

It is remarked that $f(x)$ is actually independent of x and, in particular, $f(0) \neq 0$. Furthermore, the field $g(x)$ may be written as

$$g(x) = Bx$$

with matrix B given by

$$B = -\frac{1}{h}\begin{bmatrix}1 & 0 & \cdots & 0\\-1 & \ddots & & \vdots\\\vdots & \ddots & \ddots & 0\\0 & \cdots & -1 & 1\end{bmatrix}$$

For n high enough, the piecewise linear approximation of the spatial distribution of temperature is acceptable and model (4) [or, equivalently, (5)] describes reasonably well the transport and heating phenomena inside the pipe [1].

2.1. Equilibrium states

Fig. 6 shows the state (i.e. the value of temperature distribution along the pipe) at four different times. This simulation is performed with $n = 100$, $\alpha R = 1$, $L = 100$ m, $h = 1$ m and $u(t)$ is a decreasing step with initial value 100 and final value 25, the transition occurring at $t = 1$ *s*. The absolute values of temperature and radiation have no physical meaning and they should be understood as normalised values. What is important to notice in the result expressed by Fig. 6 is the shape of the equilibrium distribution of oil temperature under a constant flow and radiation and the way it evolves in the presence of a flow change. As seen in Fig. 6(a), under a constant flow (and in the presence of constant radiation), the temperature

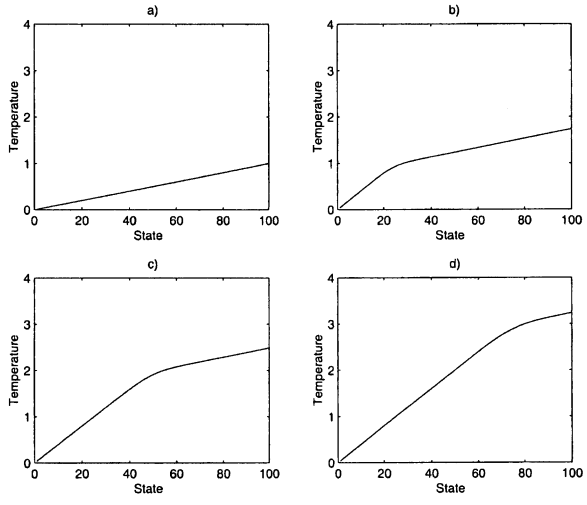

Fig. 6. System state in four time instants after a decrease in oil flow: (a) $t = 1$ s, (b) $t = 2$ s, (c) $t = 3$ s, (d) $t = 4$ s.

increases along the pipe as a straight line. This assumes that losses to the environment are neglegible. Losses cause a temperature decrease and, consequently, a "bending" downwards of the curve expressing spatial temperature distribution. In the presence of losses, this would no longer be a straight line. The oil pipe in the ACUREX field of Plataforma Solar de Almeria is inside a glass pipe (seen in Fig. 3 as the "white rods"). This causes a green-house effect, thereby greatly reducing losses. Since the main purpose of this paper is control design with a model as simple as possible, losses will be neglected hereafter.

The above discussion may be formalised as follows. The system described by (1) will reach an equilibrium state when, for all $z\epsilon[0,L]$ the partial derivative of temperature with respect to time vanishes. From (1) it is seen that for constant u and αR, equilibrium temperature distributions are given by

$$T(z,t) = T(0,t) + \int_0^z \frac{\alpha R}{u} \mathrm{d}z' = T(0,t) + \frac{\alpha R}{u} z$$

i.e. they are straight lines in space. A similar conclusion applies to the space discretized system (4). The details are ommited.

2.2. Reachable states

Characterising the set of reachable states (spatial temperature distributions) is of interest because it provides the ground for the approximate model used in Section 4 as a basis for control design. Indeed, the arguments below show that the only possible spatial temperature distributions are monotonically increasing in space. Furthermore, the temperature values are bounded.

The set of reachable states depends on the constraints imposed on the flow (manipulated input) and solar radiation (disturbance input). These are given by

$$0 < u_{\min} < u(t) < u_{\max} \tag{6}$$

and

$$0 < R_{\min} < R(t) < R_{\max} \tag{7}$$

In the ACUREX field of Plataforma Solar de Almeria the minimum value of the flow results from safety considerations and is given by $u_{\min} = 2$ l/s. The maximum depends on the value yielded by the pump, being given by $u_{\max} = 9$ l/s. The radiation is clearly always positive and bounded by a value corresponding to a perfectly bright summer day. Below $R = 100$ W/m^2 the field is automatically stopped for safety reasons, so that a minimum value for radiation has also to be considered. It should be added that thre oil temperature must be below the maximum value of 290°C which is imposed by safety reasons.

The characterisation of the reachable set of states of model (1) is performed in two steps. In the first step, the space derivative of T for $z = 0$ (collector's input) is computed. In the second step, it is shown that the signal $\Gamma = \frac{\partial T}{\partial z}$ propagates along the pipe with a velocity equal to the oil velocity. The conjunction of both these steps allows one to conclude that the temperature has always a finite derivative. This in turn implies that $T(z,t)$ is a continuous function. It is remarked that the derivative may not itself be continuous.

If T_{in} and R are constant, then the set of reachable states of (1) is the set of continuous functions in the interval $[0,L]$ with minimum and maximum values of the derivative given, respectively, by $\frac{\alpha R}{u_{\max}}$ and $\frac{\alpha R}{u_{\min}}$.

Consider now the finite dimensional approximation (5). Let M be the state space associated with (5). In this case $M = R^n$. The reachability algebra C of (5) [13] is the smallest Lie algebra of vector fields in M containing f and g. It is shown in [13] that any element of C is a linear combination of the vector fields generated by taking successive Lie brackets of f and g. In this way, it is easy to show that any element of C is generated by the linear combination of the three following vectors:

$$\begin{bmatrix} 1 \\ 1 \\ \vdots \\ 1 \end{bmatrix} \quad \begin{bmatrix} 1 \\ 0 \\ \vdots \\ 0 \end{bmatrix} \quad Bx$$

These vectors represent the directions along which the state x may be changed. The first vector concerns heating by solar radiation. Oil is heated uniformly along the pipe and this corresponds to a state trajectory in the direction $[1,\ldots,1]^T$. The second vector corresponds to the fact that it is possible to manipulate the derivative of temperature with respect to space at the pipe inlet. Finally, the third vector represents oil transport along the pipe.

The finite dimensional system is non-controllable since it is not possible to reach the whole state-space. For instance (as in the distributed parameter model) it is not possible to reach a distribution of temperature which decreases along the pipe.

3. Feedback linearization

It is possible to show that system (5) is input to state linearizable only for $n = 1$ and $n = 2$ [2]. This will not be pursued here. Instead, input–output exact linearization is considered [21,9].

3.1. Input–output linearization

Input–output exact linearization consists of finding a state transformation (diffeomorphism)

$$z = \Phi(x)$$

and input transformation

$$u = \frac{v - b(x)}{a(x)}$$

where v is the transformed input and $a(\cdot)$, $b(\cdot)$ are convenient state functions (to be made precise below), such that the transformed system has the form

$$\begin{aligned} \dot{z}_1 &= z_2 \\ \dot{z}_2 &= z_3 \\ &\vdots \\ \dot{z}_{r-1} &= z_r \\ \dot{z}_r &= v \\ \dot{z}_{r+1} &= q_{r+1}(z) \\ &\vdots \\ \dot{z}_n &= q_n(z) \\ y &= z_1 \end{aligned} \tag{8}$$

where $y = h(x)$ is the system output and r is the so called relative degree. In this transformed form, the relation between the new input v and the output is an integrator of order r. The last n–r equations correspond to unobservable states and they must be shown to be stable.

Consider the system defined by (4) with the output defined by

$$y = h(x) = x_n \tag{9}$$

The relative degree [21,9] is given by the number of times the output y has to be differentiated at a given time t_0 so that $u(t_0)$ explicitely appears. Differentiating the output given by (9) one obtains:

$$\dot{y} = \dot{x}_n = \alpha R - \frac{x_n - x_{n-1}}{h} u$$

and it is concluded that the relative degree of this system is $r = 1$. The transformation $z = \Phi(x)$ which brings the system to the form (8) is thus of the form

$$z = \Phi(x) = \begin{bmatrix} h(x) \\ \phi_2(x) \\ \vdots \\ \phi_n(x) \end{bmatrix} \tag{10}$$

with convenient functions $\phi_2, ..., \phi_n$. The linearizing control law is given by

$$u = \frac{-L_f h(x) + v}{L_g h(x)} = \frac{\alpha R - v}{x_n - x_{n-1}} h \tag{11}$$

where v is the input of the linearised system.

Eq. (11) provides a transformation such that, from the transformed input v to the output y, the dynamics reduces to a pure integrator. Once v is found with an appropriate control law, the actual control u to apply to the plant is computed from v by (11). It is remarked that this computation requires the values of the states x_n and x_{n-1} which must be available for measurement. The measure of x_{n-1} is not available in the plant considered for values of $n > 1$. In general, one possibility would be to estimate this variable. Another line of work, which is the one exploited in this paper, consists in using approximate models.

3.2. Internal dynamics

With the above control strategy it remains to show that the internal dynamics is stable. For the solar collector plant at hand, a convenient way for studying internal dynamics is by considering tracking dynamics [9]. Let the initial condition $x^0 = x(0)$ be compatible with the reference signal $y_r(t)$. This means that

$$\begin{aligned} y_r(0) &= h(x^0) \\ y_r^{(1)}(0) &= L_f h(x^0) \\ &\vdots \\ y_r^{(r-1)}(0) &= L_f^{r-1} h(x^0) \end{aligned}$$

The tracking manifold is defined by

$$M_t = \left\{ x \in M : h(x) = y_r(t), ..., L_f^{r-1} h(x) = y_r^{(r-1)}(t) \right\}$$

where M is the state-space. The tracking dynamics is the dynamics of the system constrained to M_t. It corresponds to the internal dynamics when the output is perfectly tracking $y_r(t)$. Finding the internal dynamics in general involves computing Φ which, in this case, requires a cumbersome numerical computation. So, here, only significant special cases are considered. Fig. 7 shows the internal dynamics when the initial state is a straight line added to a sinusoid with a period equal to the length of the pipe. Normalised variables are used. As seen in this picture, although the input and output temperatures are constant, intermediate values of the state present a noticeable oscillation. By choosing another initial condition, a different internal dynamics is yielded. Fig. 8 shows another example in which the oscillations have a spatial period equal to $L/3$.

3.3. Internal dynamics with approximate control laws

The change of input variable (11) leads to a relation between the transformed input v and the output y exactly given by an integrator. It happens, however, that in the ACUREX field of Plataforma Solar de

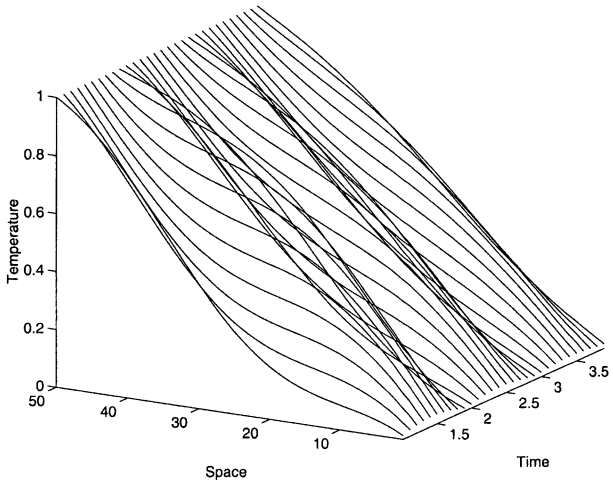

Fig. 7. Example of internal dynamics. Normalized variables are used.

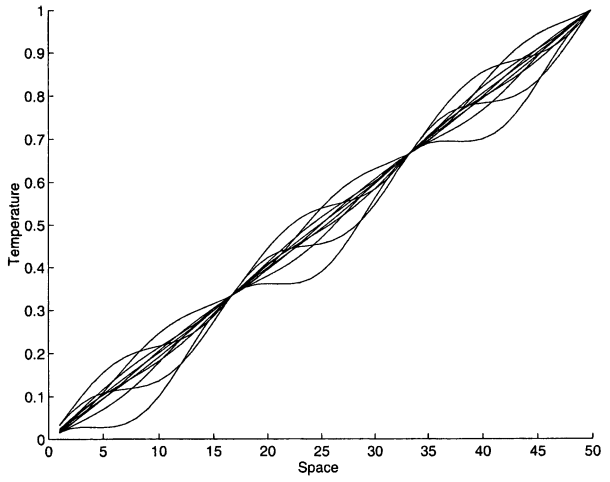

Fig. 8. Another example of internal dynamics. Each curve corresponds to the spatial temperature distribution at a time. Normalized variables are used.

Almeria (PSA), while $y = x_n$ is available for measurement, x_{n-1} is in general not. Indeed, only the inlet oil temperature is available for measurement.

In this realm, one issue with practical incidence to consider is plant internal dynamics when (11) is replaced by

$$u = \frac{\alpha R - v}{T(L, t) - T(L - d, t)} \tag{12}$$

where d is the distance between both temperature sensors.

Figs. 9 and 10 correspond to the situations in which $d = L/n$ (the one corresponding to exact input-output linearization) and $d = L$ (the one found at PSA). The value of n is taken $n = 100$. Each of these figures show the time evolution of the state components, starting from a given initial condition.

Start by considering Fig. 9. The output temperature, corresponding to the component initialized at 1 (i.e. the upper curve) is constant. This is what should be expected,

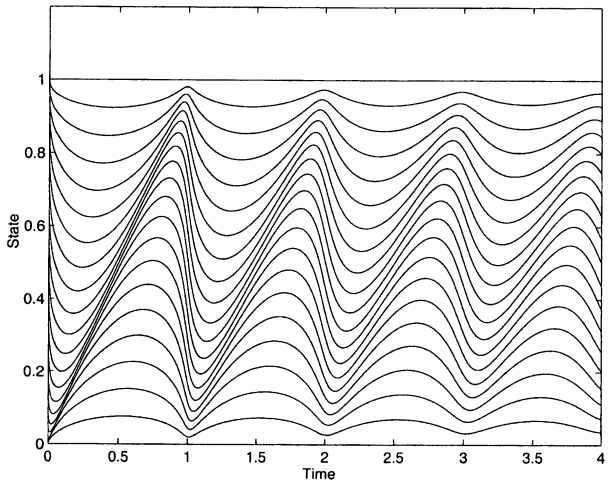

Fig. 9. Internal dynamics with $d = L/n$. Normalized variables are used.

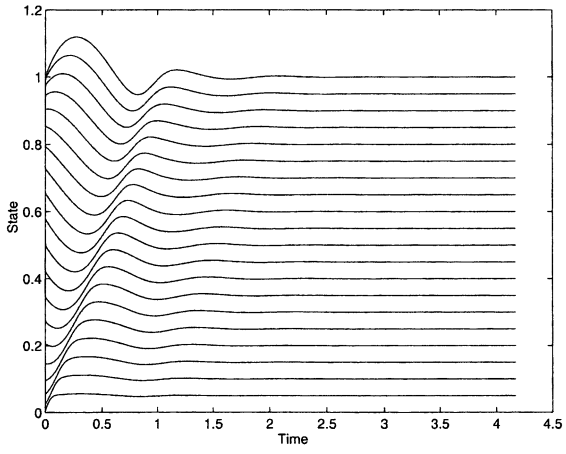

Fig. 10. Internal dynamics with $d = L$. Normalized variables are used.

since $v = 0$ and the relation between v and y is exactly an integrator. The other states, according to the previous discussion on internal dynamics, present oscillations.

Consider now Fig. 10. The output is no longer constant and there is an initial transient which is explainable by the fact that the control transformation used is now only an approximation to the linearizing one. It is to be remarked that internal oscillations are much smaller in this case.

4. Control design with an approximate model

Motivated by the discussion on the previous section, control is now designed on the basis of the model:

$$\dot{y} = -u(y - y_0)\frac{1}{L} + \alpha R \tag{13}$$

where y is the outlet oil temperature, y_0 is the inlet oil temperature and u is the oil flow velocity. The resulting equations may be interpreted by taking $n = 1$.

In (13) the optical efficiency α is not exactly known in advance and, furthermore, it includes modeling errors, being expected to change slowly. It is thus to be estimated. Let α denote the true optical efficiency, $\hat{\alpha}$ an estimate of α and $\tilde{\alpha}$ the difference between the two:

$$\tilde{\alpha} = \alpha - \hat{\alpha} \tag{14}$$

Then (13) yields

$$\dot{y} = -u(y - y_0)\frac{1}{L} + (\hat{\alpha} + \tilde{\alpha})R \tag{15}$$

From (12) the virtual control signal v is given by

$$v = -u(y - y_0)\frac{1}{L} + \hat{\alpha}R \tag{16}$$

This may now be used to control the outlet oil temperature by using a linear controller. The actual control signal applied to the plant is given by

$$u = \frac{\hat{\alpha}R - v}{y - y_0}L \tag{17}$$

Inserting (17) in (15) yields

$$y = v + \tilde{\alpha}R \tag{18}$$

Eq. (17) defines the static transformation Ψ such that between the variables v and y the model dynamics is equivalent to a linear system (integrator), disturbed by an input offset with an unknown gain.

4.1. Design of joint adaptation and control

In order to obtain an adaptation law for updating $\hat{\alpha}$, an argument based on the Lyapunov's direct method [21,10] is used. For that sake, consider the candidate Lyapunov function defined by

$$V(e, \tilde{\alpha}) = \frac{1}{2}(e^2 + \frac{1}{\gamma}\tilde{\alpha}^2) \tag{19}$$

where $\gamma > 0$ is a constant parameter and e is the tracking error defined by

$$e(t) = y_r - y(t) \tag{20}$$

y_r being a constant set-point. Since the linearised system is an integrator, there is no need to include integral action in the controller. Thus, let the control in continuous time be given by the PD law

$$v = k_p e - k_d \dot{y} \tag{21}$$

with k_p and k_d constant gains. Replacing this control law in the transformed plant Eq. (18), yields the following closed loop model

$$\dot{y} = \frac{k_p}{1 + k_d}e + \frac{R}{1 + k_d}\tilde{a} \tag{22}$$

For V to be a Lyapunov function, its time derivative must be nonpositive. Assuming a constant set-point and a constant α, use (14), and get

$$\dot{V} = -e\dot{y} - \frac{1}{\gamma}\tilde{\alpha}\dot{\hat{\alpha}} \tag{23}$$

Upon using (22), this becomes

$$V = -\frac{k_p}{1 + k_d}e^2 - [\frac{R}{1 + k_d}e + \frac{1}{\gamma}\dot{\hat{\alpha}}]\tilde{\alpha} \tag{24}$$

The adaptation law for $\hat{\alpha}$ is chosen such that the term multiplying $\tilde{\alpha}$ above vanishes:

$$\dot{\hat{\alpha}} = -\frac{\gamma}{1 + k_d}Re \tag{25}$$

With this choice, $\dot{V}$ is negative semidefinite if $k_p > 0$ and $k_d > -1$. Furthermore, by LaSalle's invariance theorem [21], all the trajectories converge to the maximum invariant set where $\dot{V} = 0$, implying that

$$\lim_{t \to \infty} y(t) = y_r \tag{26}$$

This last conclusion applies only to the simplified model.

5. Experimental results

The control strategy previously described was tested in the ACUREX field. Two kinds of tests were performed. In the first experiment only the linearizing feedback loop is closed. The objective is to assess the viability of the simplifications introduced by analyzing the response to the input v. In the second experiment, a linear proportional-derivative (PD) controller was included together with the adaptation of α.

5.1. Experiment 1

The aim of experiment 1 is to show that, from the virtual control signal v to y, the system behaves approximatelly as an integrator, even in the presence of strong disturbances in solar radiation. Therefore in this experiment only the linearizing loop is closed. The results are seen on Figs. 11–14. The system is driven by a rectangular virtual control signal with varying amplitudes

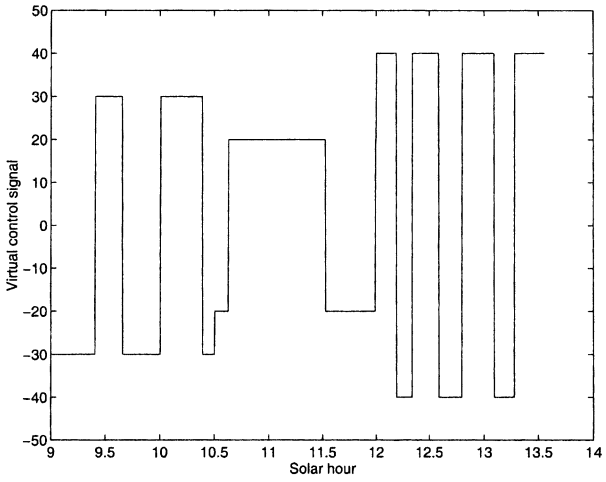

Fig. 11. Experiment 1: virtual control signal.

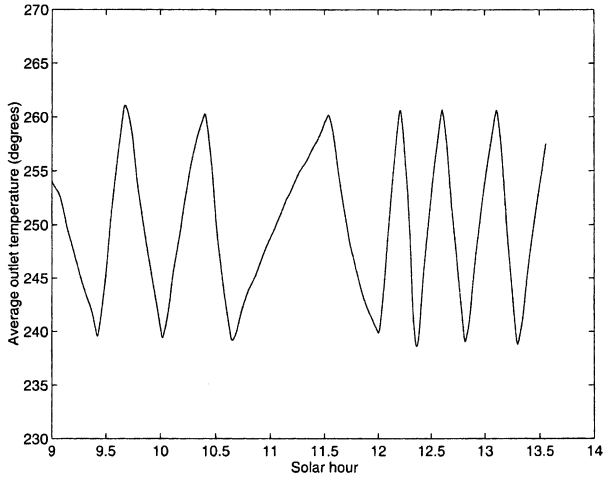

Fig. 12. Experiment 1: average outlet temperature.

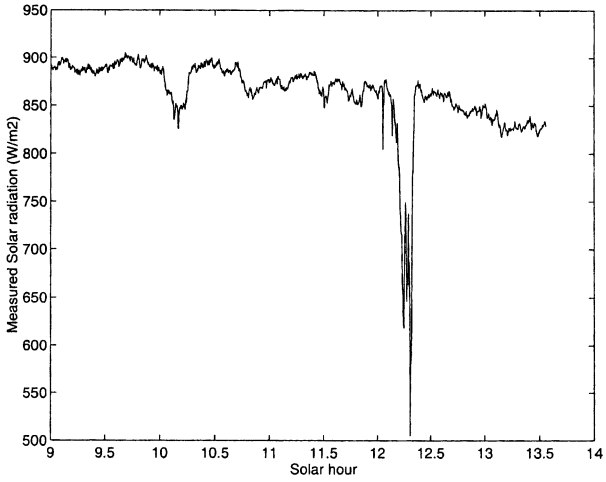

Fig. 13. Experiment 1: solar radiation.

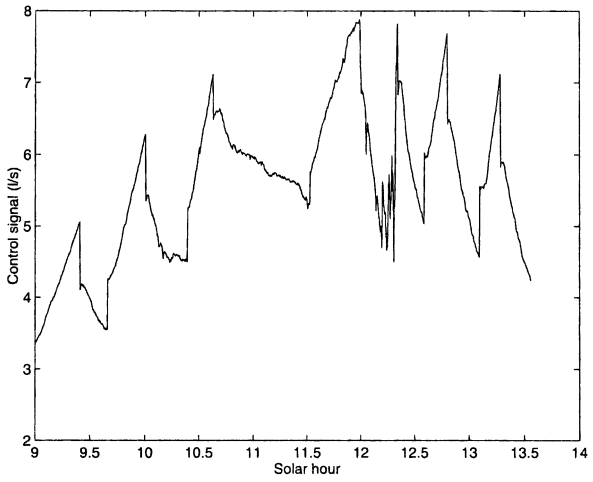

Fig. 14. Experiment 1: actual control signal applied to the plant.

and duration (Fig. 11). As expected, a saw-tooth like temperature signal results by integrating the piecewise constant virtual input. This actually happens, as seen in Fig. 12 which shows the outlet oil temperature varying approximately as a triangular signal with different slopes depending on the amplitude of the virtual control (Fig. 11). Some discrepancies are explainable by the error in the value of the estimate used for α, in accordance with Eq. (18). By using a better estimate, as would happen if an adaptive scheme is used (as in experiment 2 below), an even better approximation to the integrator would be obtained. It can also be seen that the sudden reduction in solar radiation (Fig. 13) is almost not sensed in the output since the actual control signal compensates for it (Fig. 14).

5.2. Experiment 2

In experiment 2, the outer-loop is closed so as to track a temperature reference. The virtual control signal v is generated by the following discrete time version of the PD controller (21):

$$v(k) = k_p e(k) + k_d(y(k) - y(k-1)) \tag{27}$$

The transformed control signal (actually applied to the plant) is computed from v by:

$$u(k) = \frac{\hat{\alpha}(k)R(k) - v(k)}{y(k) - y_0(k)}h \tag{28}$$

with the estimate $\hat{\alpha}$ updated by the following approximation to (25):

$$\hat{\alpha}(k+1) = \alpha(k) - k_a \mathrm{Re}(k) \tag{29}$$

A sampling time of 15 s and the following gains are used:

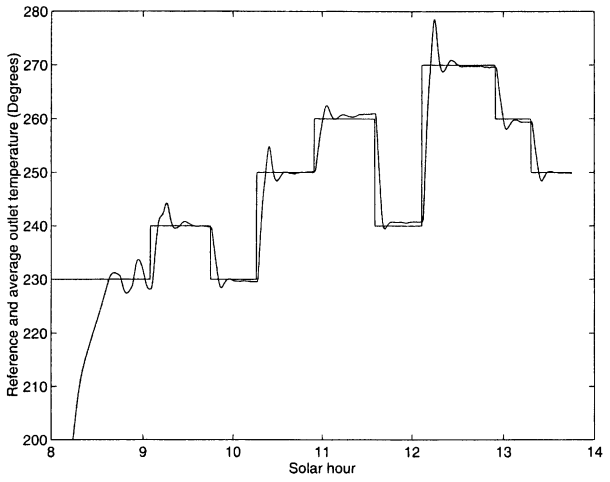

Fig. 15. Experiment 2: reference temperature and average outlet temperature.

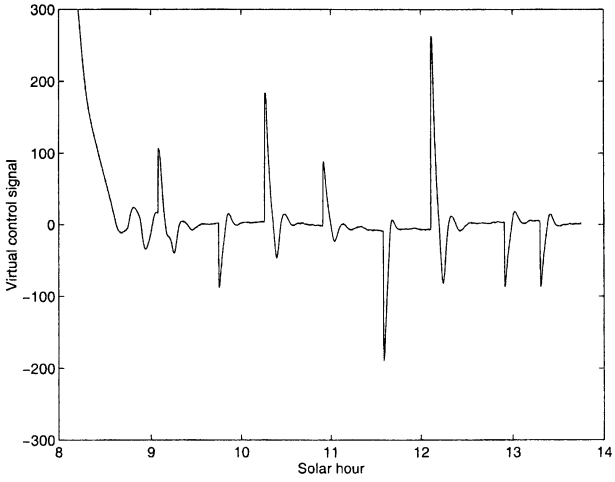

Fig. 16. Experiment 2: virtual control signal.

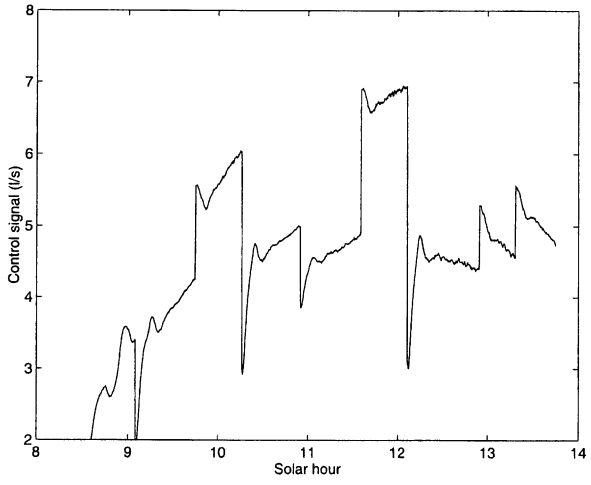

Fig. 17. Experiment 2: actual control signal applied to the plant (flow).

$k_p = 9, k_a = .0001/820, k_d = 15$

During the experiment the radiation was roughly constant, its mean value of 820 Wm^{-2} being lumped in the constant k_a. Fig. 15 shows the reference temperature and average outlet temperature taken over all the 10 field loops. Overshoot in positive steps could be reduced by using lower gains. Fig. 16 shows how the virtual control signal goes to approximately zero as the outlet temperature approximates the setpoint, as would be expected in controlling a true linear integrator system. Fig. 17 shows the actual control applied to the plant.

6. Conclusions

The control of a distributed collector solar field has been addressed. The approach followed relies on an adaptive nonlinear controller designed on a basis of a plant reduced complexity model. This model directly stems from a distributed parameter model expressing the physical phenomena involved. Thus, the control design procedure is expected to be applicable to other processes with a similar structure, in particular plug-flow chemical reactors.

For justifying the simplifications assumed, the following studies were performed. First, a comparison with the input–output feedback linearizing control resulting from a much higher order model was made. It was concluded that the structure of both transformations (the ones resulting from the high order model and the simplified model) are the same, with a different placement of one temperature sensor. The placement corresponding to the simplified model is the one actually found in the plant used for experimental tests and hence its interest. The internal dynamics corresponding to both cases were studied by simulation.

On the other hand, an experiment performed on the actual plant shows that the reduced complexity model leads to a reasonable approximation of an integrator.

Once the model is justified, another experiment illustrates the use of a Lyapunov based adaptive controller for tackling uncertainty in collector optical efficiency.

This procedure has been shown to be a viable method for the control of this kind of processes. Its practical implementation is simple, while achieving a good approximation to the exact adaptive controller.

Open issues include a stability proof which takes into account the true plant model and the estimation of the temperature needed for exact feedback linearization from available plant measurements.

References

[1] A.C. Bajpai, I.M. Calus, J.A. Fairley, Numerical Methods for Engineers and Scientists. John Wiley & Sons, 1977.

[2] M. Barão, Dynamics and Nonlinear Control of a Solar Collector Field. Thesis (in Portuguese), Universidade Técnica de Lisboa, Instituto Superior Técnico, Lisboa, Portugal, 2000.
[3] M. Berenguel, E. Camacho, Frequency based adaptive control of systems with antiressonance modes. Prep. 5th IFAC Symp. Adaptive Systems in Control and Signal Processing. Budapest, Hungary, 1995, pp. 195–200.
[4] M. Berenguel, Contributions to the Control of Solar Collector Systems (in Spanish), PhD. thesis, University of Sevilla, Spain, 1995.
[5] E.F. Camacho, F.R. Rubio, J.A. Gutierrez, Modelling and simulation of a solar power plant with a distributed collectors system. Proc. IFAC Symp. Power Syst. Mod. and Control Appl., Brussels, Belgium 1988, pp. 11.3.1–11.3.5.
[6] E.F. Camacho, M. Berenguel, C. Bordóns, Adaptive generalized predictive control of a distributed collector field, IEEE Trans. Contr. Syst. Tech. 2 (4) (1994) 462–467.
[7] E.F. Camacho, M. Berenguel, F. Rubio, Application of a gain scheduling generalized predictive controller to a solar power plant, Control Eng. Practice 2 (2) (1994) 227–238.
[8] F. Coito, J.M. Lemos, R.N. Silva, E. Mosca, Adaptive control of a solar energy plant: exploiting accessible disturbances, Int. J. Adapt. Control Signal Process 11 (1997) 327–342.
[9] A. Isidori. Nonlinear Control Systems, 2nd Edition, Springer-Verlag, 1995.
[10] P. Kokotovic, M. Krstic, Adaptive nonlinear control: a Lyapunov approach, in: K Judd, A. Mees, K.L. Teo, T.L. Vincent (Eds.), Control and Chaos, Birkhauser, 1997, pp. 170–182.
[11] D.J. Leith, W.E. Leithead, Survey of gain-scheduling analysis and design, Int. J. Control 73 (11) (2000) 1001–1025.
[12] A. Meaburn, F.M. Hughes, Resonance characteristics of a distributed solar collector fields, Solar Energy 51 (3) (1993) 215–221.
[13] H. Nijmeijer, A.J. van der Schaft, Nonlinear Dynamical Control Systems, Springer-Verlag, 1990.
[14] A. Orbach, C. Rorres, R. Fischl, Optimal control of a solar collector loop using a distributed-lumped model, Automatica 27 (3) (1981) 535–539.
[15] L. Rato, J.M. Lemos, E. Mosca, Integrating predictive and switching control: basic concepts and an experimental case study, in: F. Allgöwer, A. Zheng (Eds.), Nonlinear Model Predictive Control, Birkhäuser Verlag, Basel, Boston, Berlin, 2000, pp. 181–190.
[16] C. Rorres, A. Orbach, R. Fischl, Optimal and suboptimal control policies for a solar collector system, IEEE Trans. Autom. Control, AC-25 6 (1980) 1085–1091.
[17] F. Rubio, M. Berenguel, E. Camacho, Fuzzy logic control of a solar power plant, IEEE Trans. on Fuzzy Systems 3 (4) (1995) 459–468.
[18] S. Sastry, A. Isidori, Adaptive control of linearizable systems, IEEE Trans. on Automatic Control 34 (11) (1989) 1123–1131.
[19] J. Seinfeld, G. Gavalas, M. Hwang, Control of plug-flow tubular reactors by variation of flow rate, Ind. Eng. Chem. Fundam. 9 (4) (1970) 651–655.
[20] R.N. Silva, L.M. Rato, J.M. Lemos, F. Coito, Cascade control of a distributed collector solar field, J. Proc. Cont. 7 (2) (1997) 111–117.
[21] J. Slotine, W. Li, Applied Nonlinear Control, Prentice Hall, 1991.
[22] Y. Takahashi, C.S. Chang, D.M. Auslander, Parametere-instellung bei linearen DDC-Algorithmen, Regelungstechnik und Process-Datenverarbeitung 19 (1971) 237–244.